

## AC magnetic-field response of the ferromagnetic superconductor $\text{UGe}_2$ with different magnetized states

Hiroyuki Tanaka, Akira Yamaguchi,\* Ikuto Kawasaki, and Akihiko Sumiyama

*Graduate School of Material Sciences, University of Hyogo, 3-2-1 Kouto, Kamigoricho, Ako-gun, Hyogo 678-1297, Japan*

Gaku Motoyama

*Graduate School of Material Science, Shimane University, Matsue, Shimane 690-8504, Japan*

Tomoo Yamamura

*Institute for Materials Research, Tohoku University, Sendai, Miyagi 980-8577, Japan*



(Received 18 July 2017; revised manuscript received 11 January 2018; published 29 January 2018)

We have performed parallel measurements of dc-magnetization and ac-magnetic susceptibility for a ferromagnetic superconductor,  $\text{UGe}_2$ , in the ferromagnetic-superconducting phase. dc-magnetization measurements revealed that adequate demagnetizing of the sample allows for the preparation of various magnetized states with different zero-field residual magnetization. We observed that these states exhibit varying ac superconducting response at large ac-field amplitudes. The amount of ac flux penetration is less in the demagnetized state involving many domain walls. This result seems to contradict the theory that considers the domain walls as weak links. Moreover, the ferromagnetic domain walls enforce the shielding capability of superconductivity. This observation sheds light on the role of the domain walls on superconductivity, which has been a controversial issue for several decades. Two possible scenarios are presented to explain the enhancement of the shielding capability by the domain walls.

DOI: [10.1103/PhysRevB.97.020509](https://doi.org/10.1103/PhysRevB.97.020509)

The uranium compound  $\text{UGe}_2$  has attracted considerable attention since the discovery of the coexistence of ferromagnetic ordering and superconductivity in its high-pressure and low-temperature phase [1], which has been a long-standing target in the unconventional-superconductors science. This finding has caused many researchers to discover a similar ferromagnetic (FM) superconducting (SC) phase in related uranium compounds such as  $\text{UCoGe}$  [2] and  $\text{URhGe}$  ([3], and references therein).

In FM and SC uranium compounds, the itinerant  $f$  electrons are responsible for both the properties. Due to large exchange splitting, a spin-triplet pairing is theoretically suggested [4–10]. Furthermore, the large anisotropy and strong internal field are considered to contribute to the formation of the equal-spin-pairing and nonunitary SC state. In the latter, the amplitudes of the order parameters are different between spin-up and spin-down pairs ( $\Delta_{\uparrow\uparrow} \neq \Delta_{\downarrow\downarrow}$ ). In an extreme scenario, the  $A_1$ -like phase is proposed, which is a similar phase to the  $A_1$  phase observed in superfluid  $^3\text{He}$ . In the  $A_1$ -like phase, only the spin-up pairs exist, while the spin-down band remains in the normal state.

The relation between the SC order parameters and the magnetic-domain structure that is inherent in the FM phase has also been discussed in many theoretical studies [5,6,9–12]. The order parameters are expected to strongly couple with the direction of magnetization. In case of the  $A_1$ -like phase, the state with finite  $\Delta_{\uparrow\uparrow}$  ( $\Delta_{\downarrow\downarrow}$ ) occurs at the domain with the

positive (negative) magnetization  $M$ . According to Mineev, the different magnetic domains with  $\pm\mu_0 M$  are normally related to the *equivalent* order parameter  $\Psi$  and  $i\Psi^*$ , respectively [6]. Fomin indicated that the magnetic-domain walls are regarded as weak links for the superconductivity [5]. Further, Mineev presented a formalism of Josephson current across the domain wall [9,10]. Conversely, some phenomenological theories have predicted enhanced superconductivity at the domain walls [11,12].

In contrast to the extensive theoretical studies that have been performed, experimental investigations focusing on the relation between superconductivity and domain structure are few. The research carried out by Hykel and co-workers on  $\text{UCoGe}$  using scanning  $\mu$ -superconducting quantum interference device (SQUID) magnetometry are an exception [13–15]. In this research, the authors observed that the Meissner-Ochsenfeld effect occurs independently for each magnetic domain.

Notably, the authors commented in the same paper that the self-induced vortex state is realized in  $\text{UCoGe}$  [13,15]. Deguchi *et al.* [16] also suggested a similar viewpoint. From a mesoscopic point of view, the SC phase of the FM compounds cannot be in the Meissner state because the internal field resulting from a large FM magnetization  $M = \pm\mu_0 M_f$  ( $M_f$  is the saturation magnetization) exceeds the lower critical field  $\mu_0 H_{c1}$ , which is in the order of less than  $100 \mu\text{T}$ . To realize the SC phase under such a strong magnetic field, a self-induced vortex state like a mixed state of the type-II superconductors is inevitably reached. As shown in Fig. 1(a), the domains with positive and negative  $M$  involve vortices and antivortices, respectively. Although some electromagnetic

\*yamagu@sci.u-hyogo.ac.jp

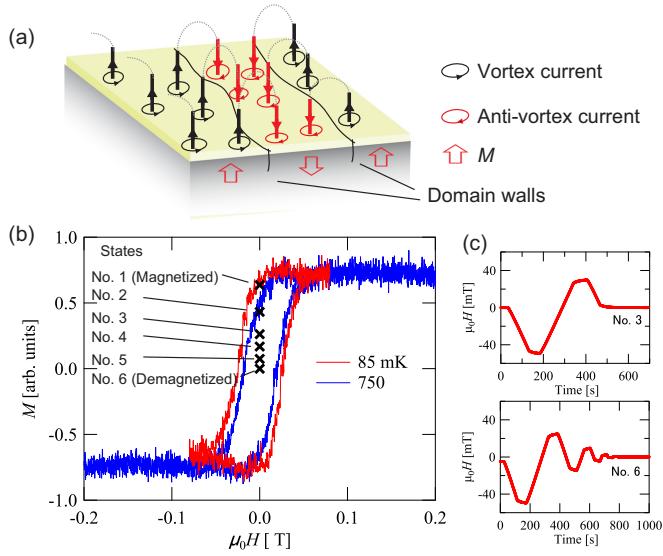


FIG. 1. (a) A schematic of the self-induced vortex state with FM domains. Effective fields due to the FM magnetization  $M$  produce SC vortex and antivortex currents in each domain. (b)  $M$ - $H$  curves of  $\text{UGe}_2$  at 750 and 85 mK. The markers represent residual magnetizations for the states prepared by different demagnetization processes. For details, see the text. (c) Examples of the sequence (No. 3 and No. 6).

considerations have been described for FM superconductors [17,18], the SC nature of such a *staggered* vortex state has not been experimentally investigated.

In this regard, we performed simultaneous measurements of dc-magnetization and ac-magnetic susceptibility in the FM-SC phase of  $\text{UGe}_2$ . The dc-magnetization measurements provided us with information regarding FM magnetization that is closely related with its domain structures. By measuring the SC ac-field response while monitoring the magnetization, the effect of the FM domain walls on the SC properties was revealed. Thus, a dependence of the SC ac-field response on the domain structure was established.

$\text{UGe}_2$  crystallizes into the orthorhombic  $Cmmm$  space group. The magnetic easy axis is along the  $a$  axis. The exchange field  $H_{\text{ex}}$  is reported to be of the order of several tens of tesla. The FM ordered moment is  $1.5\mu_{\text{B}}/\text{U}$  at ambient pressure and approximately  $1\mu_{\text{B}}/\text{U}$  in the SC region around 1.0 GPa. Owing to the large anisotropy there are only two types of magnetic domains with positive and negative  $M$  along the direction of the  $a$  axis. The electromagnetic field  $\mu_0 H_{\text{em}} (= \mu_0 M_f)$  is approximately  $\pm 0.2$  T in each domain. The domain size is reported to be of the order of several micrometers [19].

The single crystals were prepared by Czochralski technique. The residual resistivity ratio  $\rho(300 \text{ K})/\rho(2 \text{ K})$  amounts to 180. The size of the crystal used in the measurements was  $2.98 \times 0.325 \times 1.29 \text{ mm}^3$ . The demagnetization factor  $N$  was estimated as 0.124. To apply the pressure, a NiCrAl-BeCu piston-cylinder-type pressure cell was used. The applied pressure was determined from the SC transition temperature of pure indium cut to the same shape as that of the sample. A pressure of 1.15 GPa was set, which is just below the optimal pressure  $P_x = \sim 1.2$  GPa [3]. The same indium sample was used for calibrating the ac magnetometer.

Magnetic measurements were carried out using two types of magnetometers: one comprising a Hall device and the other comprising a SQUID sensor. The Hall device, a commercial product fabricated using GaAs, was settled as close to the sample as possible to measure the FM dc magnetization. Furthermore, the magnetometer based on the SQUID sensor was used to measure the ac-field responses related to the SC transition. The details of the magnetometers are described in Ref. [20]. The directions of the dc and ac magnetic fields were both along the easy axis.

Figure 1(b) shows the  $M$ - $H$  curves measured by the Hall device at 1.15 GPa. As described later, as the SC transition temperature  $T_{\text{SC}}$  was determined as 0.6 K, the curves at 750 and 85 mK can be attributed to the FM and FM-SC phases, respectively. It is worth noting that the hysteresis loop due to the FM moment remains virtually unchanged even in the FM-SC phase, which is consistent with the previous reports on  $\text{UGe}_2$  and  $\text{UCoGe}$  [13,16]. Although a slight decrease in dc magnetization was detected in the SC phase in the case of  $\text{UCoGe}$  [13,16], we could not observe any reduction in dc magnetization for  $\text{UGe}_2$  within the experimental error threshold. This is most likely due to the FM magnetization of  $\text{UGe}_2$  ( $\sim 1\mu_{\text{B}}/\text{U}$ ) being much larger than that of  $\text{UCoGe}$  ( $\sim 0.05\mu_{\text{B}}/\text{U}$ ).

In Fig. 1(b), we plot residual magnetizations at  $\mu_0 H = 0$ , obtained by applying different demagnetization processes. The states with different residual magnetization are numbered from 1 to 6, where No. 1 corresponds to the most magnetized state and No. 6 to the most demagnetized state. Examples of the demagnetization process are shown in Fig. 1(c). From the experiments, we observed that the desired residual magnetization could be set by defining the proper demagnetization process. States with the different residual magnetizations are considered to possess different domain structures: the demagnetized state would possess the finest domain structure, whereas the magnetized one is close to the single domain state. We performed ac susceptibility measurements for these magnetized and demagnetized states.

Figure 2 shows ac susceptibilities (10 Hz) for the magnetized and demagnetized states. The applied ac-field amplitude  $\mu_0 H_{\text{ac}}$  varied up to 0.625 mT. The contribution of the FM order to the ac susceptibility was small because the FM moments were almost frozen in this temperature range [21].

The perfect diamagnetism against the applied ac field was observed below 100 mK in the low-amplitude region, as previously observed by other groups [1,21]. This is indicative of a perfect shielding capability for a small ac field at the sample surface, despite the large internal dc magnetization as shown in Fig. 1(b). In the low-amplitude region, the two curves of the magnetized and demagnetized states follow each other well.

However, in the high-amplitude region, several differences were observed. First, the shielding for the ac field becomes imperfect. At  $\mu_0 H_{\text{ac}} = 0.625$  mT the fraction of the shielding is approximately 70% of the sample volume even at the lowest temperature. Second, the temperatures at which the in-phase ac susceptibility  $\chi'$  begins to drop seem to decrease. Accordingly, the peaks of the out-of-phase ac susceptibility  $\chi''$  shift to lower temperatures as  $\mu_0 H_{\text{ac}}$  increases. Thirdly, as the most remarkable feature in the high-amplitude region, the difference between the magnetized and demagnetized states becomes

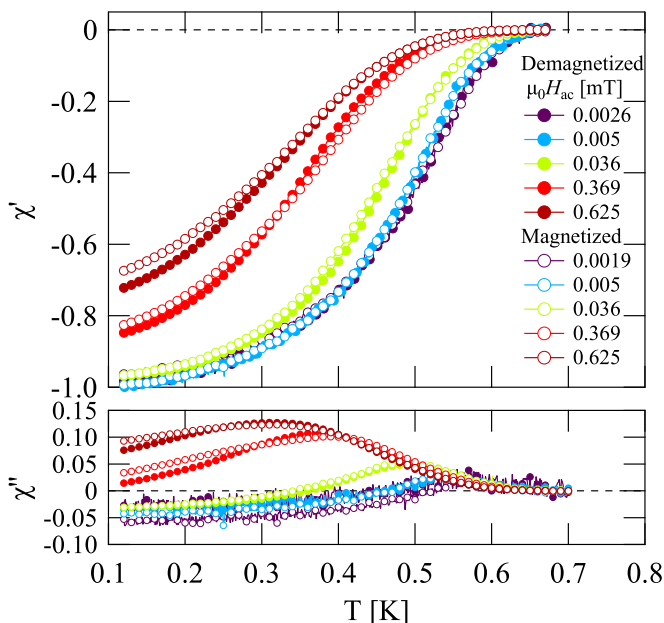


FIG. 2. Temperature dependence of ac susceptibilities of the magnetized (No. 1) and demagnetized (No. 6) states with various ac-field amplitudes.  $\chi'$  and  $\chi''$  represent in-phase and out-of-phase signals, respectively.

apparent. The shielding capability in the magnetized state seems weaker than that in the demagnetized one.

The last feature is clearly reflected in the graph displayed in Fig. 3, where the amount of the penetrating ac flux is plotted as a function of  $\mu_0 H_{ac}$ . The data were taken upon increasing  $\mu_0 H_{ac}$  continuously at a constant temperature ( $T = 80$  mK). Here the amounts of the penetrating ac flux were calculated from  $\chi'$  and a cross-section area of the sample, i.e.,  $S_{\text{sample}} = 0.42 \text{ mm}^2$ . The solid line corresponds to the full penetration of the ac flux into the sample, i.e.,  $\mu_0 H_{ac} \times S_{\text{sample}}$ , while the dotted one represents the perfect shielding. There is a systematic

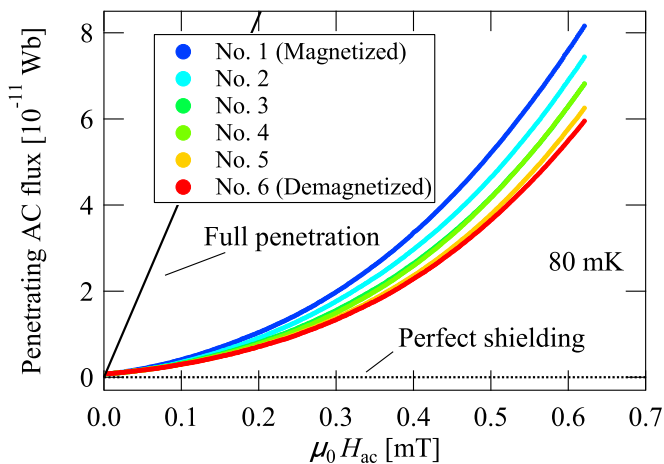


FIG. 3. Penetrating ac flux as a function of the ac-field amplitude for various magnetized states at 80 mK. The numbers of the states correspond to those in Fig. 1(b). The solid and dotted lines are the expected ones for the cases of full penetration and perfect shielding, respectively.

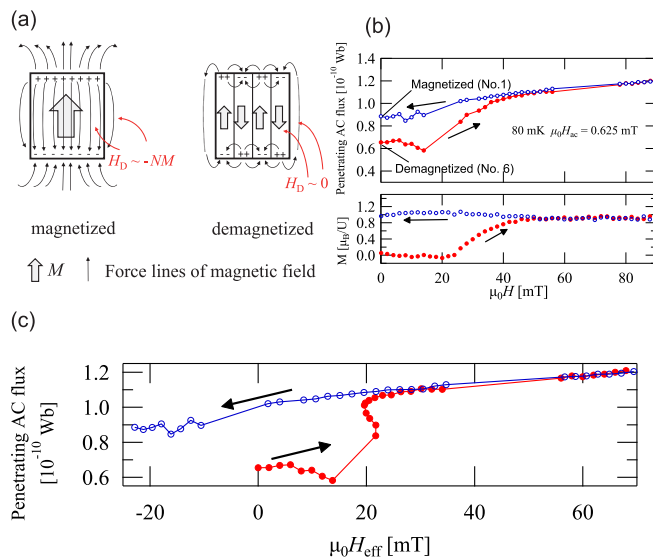


FIG. 4. (a) Domain structures and demagnetization fields for the magnetized and demagnetized states. (b) Penetrating ac flux at  $\mu_0 H_{ac} = 0.625$  mT as a function of the dc field  $\mu_0 H$ . The red, closed and blue, open circles represent the data taken in field-increasing and decreasing processes, respectively. The absence of the data around +20 mT is due to the disturbance from the SC transition of the indium reference. The lower panel shows the corresponding magnetization in each process. (c) The same data with (b) plotted as a function of the effective field,  $H_{\text{eff}} = H - NM(H_{\text{eff}})$ .

dependence of the ac shielding capability on the residual magnetization. The perfect shielding is only observed in very narrow amplitude regions lower than  $\mu_0 H_{ac} = 5 \mu\text{T}$ .

The reason for the difference between the shielding capability in the magnetized and demagnetized states cannot be explained in terms of a simple magnetostatic effect at a macroscopic scale. As shown in Fig. 4(a), the demagnetization field  $H_D$  is related to the magnetized states by  $H_D = -NM$  ( $N = 0.124$ ), while it is approximated to zero in the demagnetized sample in zero external field except in the vicinity of the surface [17,18]. The difference in  $H_D$  between the magnetized and demagnetized states is estimated to be  $-NM_f (\sim -25 \text{ mT})$  at maximum, wherein the influence of the small demagnetization field by the small SC diamagnetism can be neglected [see Fig. 1(b)].

First of all, no difference in the shielding capability in the low-ac-amplitude region was detected. If the demagnetization field was the main cause of the difference in the shielding capabilities, this would have an effect on the ac response even in the low-amplitude region. This result implies that the magnetostatic field cannot be invoked to explain such a difference.

In addition, dc-field dependence of the penetrating ac flux also cannot be explained by the influence of the demagnetization field. Figure 4(b) shows the dc-field dependence of the penetrating ac flux at the highest ac amplitude value, i.e.,  $\mu_0 H_{ac} = 0.625$  mT. The data in the lower and upper branches were measured upon increasing and decreasing the dc field, respectively. The lower panel shows the corresponding magnetization data. At every field of the upper branch the sample is almost magnetized, while in the lower branch it

is in partially magnetized states below 40 mT. Figure 4(c) shows the same data as a function of the effective field  $H_{\text{eff}} = H - NM(H_{\text{eff}})$ , in which the influence of the demagnetization field is corrected. A slight amount of distortion in the lower branch near  $H_{\text{eff}} = 20$  mT would be due to the estimation error of  $N$ . Apparently, the two branches do not follow each other even in Fig. 4(c), suggesting the difference in the shielding capability is not due to the demagnetization field.

Taken together, these results strongly suggest that the difference in the shielding capabilities seen in Fig. 3 originates from the microscopic domain structures. The influence of the magnetostatic field seems small in comparison with that of the domain structures. The little influence of the magnetostatic field is consistent with the robustness of  $T_{\text{SC}}$  against it [21], and is attributed to the nature of the triplet pairing.

The SC state of  $\text{UGe}_2$  should be the self-induced vortex state. The self-induced vortex state is identified with a spontaneously arising mixed state of the type-II superconductors. Therefore, it is worth considering the ac-field response in analogy with that of the mixed state. For strongly pinned superconductors, both external dc and ac flux lines penetrate from the surface into the sample interior [22,23]. According to the critical state model [23], the ac response can be explained with the local distribution of the depinning critical current density  $J_c$ .

Here, the experimental results seem to contradict the expectation that the domain walls are weak links. If only a small amount of Josephson current was allowed to flow across the domain walls,  $J_c$  near the domain walls should be reduced down to the maximum of the Josephson current. Then, the applied ac field could penetrate more easily with the demagnetized state because of the presence of many domain walls. In fact, in sintered high- $T_c$  superconductors [24], the flux penetration occurs in very small ac-field regions, which is attributed to the weak-link behavior of the grain boundaries. A similar behavior was reported for Fe-based superconductors [25]. The opposite tendency found in the present study suggests it should be rather the domain walls that enforce the SC shielding capability.

Two opposite scenarios can be proposed to explain this enforcement. The first is that the domain walls enhance the local  $J_c$  as additional pinning sites. Analogous behaviors have been reported for  $\text{MgB}_2$  and  $\text{Nb}_3\text{Sn}$ , in which grain boundaries

are described to function as additional pinning sites [25]. In such materials, some degradation of superconductivity occurs near the grain boundaries. However, since the quantity of the intergrain SC current is still enough, they can contribute to the superconductivity as additional pinning sites.

Another possibility peculiar to the ferromagnetic superconductors, is that the SC order parameter near the domain walls is strengthened in comparison with the domain interior. In the literature [11,12],  $T_{\text{SC}}$  near the domain wall has been discussed by the Ginzburg-Landau theory. As per research done by Samokhin and Shirokoff,  $T_{\text{SC}}$  in the vicinity of the domain wall might be substantially higher than in the bulk due to a type of microscopic electromagnetic effect [12]. Since the magnitude of the SC order parameter should be a function of  $T/T_{\text{SC}}$ , it could possibly cause an enhancement of the local  $J_c$  near the domain walls, leading to an increase of the shielding capability in the demagnetized state.

Unfortunately, it is not possible to discriminate between both the scenarios on the basis of the available data, and further experiments are required for clarification. The present results, however, indicate that if there is a difference in the SC order parameters between FM domains, it does not suppress the diamagnetic shielding current. The process of flux penetration should be complex at the domain walls, in which the vortex in one type of domain interacts with the antivortex in another type. Detailed theoretical investigations would also be required.

In summary, we detected the difference in the ac superconducting response at large ac-field amplitude among the different magnetized states of  $\text{UGe}_2$  and observed the FM-domain-dependent behavior of the SC property of  $\text{UGe}_2$ . The domain walls seemed to enforce the shielding capability rather than work as weak links. Currently, a comprehensive theory that describes the SC state with the triplet pairing in the self-induced vortex state has not been established yet. Further investigation involving the rich physics of the vortex matter in the unconventional superconductors is strongly required.

We thank Y. Hasegawa, Y. Kaneyasu, K. Machida, H. Yamagami, K. Deguchi, D. Aoki, S. E. Otabe, H. Kitano, and V. P. Mineev for valuable discussions. This study was supported by JSPS KAKENHI (Grant No. 16K05450), and carried out in the joint research in Institute for Materials Research, Tohoku University.

- 
- [1] S. S. Sexena, P. Agarwal, K. Ahllan, F. M. Grosche, R. K. W. Haselwimmer, M. J. Steiner, E. Pugh, I. R. Walker, S. R. Jullian, P. Monthoux, G. G. Lonzarich, A. Huxley, I. Sheikin, D. Braithwaite, and J. Flouquet, *Nature (London)* **406**, 587 (2000).
- [2] N. T. Huy, A. Gasparini, D. E. de Nijs, Y. Huang, J. C. P. Klaasse, T. Gortenmulder, A. de Visser, A. Hamann, T. Görlach, and H. v. Löhneysen, *Phys. Rev. Lett.* **99**, 067006 (2007).
- [3] D. Aoki and J. Flouquet, *J. Phys. Soc. Jpn.* **81**, 011003 (2012).
- [4] K. Machida and T. Ohmi, *Phys. Rev. Lett.* **86**, 850 (2001).
- [5] I. A. Fomin, *JETP Lett.* **74**, 111 (2001).
- [6] V. P. Mineev, *Phys. Rev. B* **66**, 134504 (2002).
- [7] I. A. Fomin, *J. Exp. Theor. Phys.* **95**, 940 (2002).
- [8] V. P. Mineev and T. Champel, *Phys. Rev. B* **69**, 144521 (2004).
- [9] V. P. Mineev, *J. Low Temp. Phys.* **158**, 615 (2010).
- [10] V. P. Mineev, *AIP Conf. Proc.* **1134**, 68 (2009).
- [11] A. I. Buzdin and A. S. Mel'nikov, *Phys. Rev. B* **67**, 020503(R) (2003).
- [12] K. V. Samokhin and D. Shirokoff, *Phys. Rev. B* **71**, 104527 (2005).
- [13] C. Paulsen, D. J. Hykel, K. Hasselbach, and D. Aoki, *Phys. Rev. Lett.* **109**, 237001 (2012).
- [14] D. J. Hykel, Ph.D. thesis, Université Joseph Fourier, Grenoble, 2011.
- [15] D. J. Hykel, C. Paulsen, D. Aoki, J. R. Kirtley, and K. Hasselbach, *Phys. Rev. B* **90**, 184501 (2014).
- [16] K. Deguchi, E. Osaki, S. Ban, N. Tamura, Y. Simura, T. Sakakibara, I. Satou, and N. K. Sato, *J. Phys. Soc. Jpn.* **79**, 083708 (2010).
- [17] E. B. Sonin, *Phys. Rev. B* **66**, 100504(R) (2002).

- [18] M. Fauré and A. I. Buzdin, *Phys. Rev. Lett.* **94**, 187202 (2005).
- [19] S. Sakarya, N. H. van Dijk, and E. Brück, *Phys. Rev. B* **71**, 174417 (2005).
- [20] T. Fujisawa, A. Yamaguchi, G. Motoyama, D. Kawakatsu, A. Sumiyama, T. Takeuchi, R. Settai, and Y. Onuki, *Jpn. J. Appl. Phys.* **54**, 048001 (2015).
- [21] H. Nakane, G. Motoyama, T. Nishioka, and N. K. Sato, *J. Phys. Soc. Jpn.* **74**, 855 (2005).
- [22] C. P. Bean, *Rev. Mod. Phys.* **36**, 31 (1964).
- [23] A. M. Campbell, *J. Phys. C: Solid State Phys.* **2**, 1492 (1969).
- [24] B. Ni, T. Munakata, T. Matsushita, M. Iwakuma, K. Funaki, M. Takeo, and K. Yamafuji, *Jpn. J. Appl. Phys.* **27**, 1658 (1988).
- [25] J. H. Durrell, C.-B. Eom, A. Gurevich, E. E. Hellstrom, C. Tarantini, A. Yamamoto, and D. C. Larbalestier, *Rep. Prog. Phys.* **74**, 124511 (2011).